UDC 517 . 9

STABILITY OF SHOCK WAVES IN THE MODIFIED QUINTIC COMPLEX GINZBURG – LANDAU EQUATION

СТІЙКІСТЬ УДАРНИХ ХВИЛЬ У МОДИФІКОВАНОМУ КОМПЛЕКСНОМУ РІВНЯННІ ГІНЗБУРГА – ЛАНДАУ П'ЯТОГО СТЕПЕНЯ

F. B. Pelap

Univ. Dschang
PO Box: 69 Dschang, Cameroon
e-mail: fbpelap@yahoo.fr

A. J. Kenfack

Univ. de Yaoundé I
BP 812 Yaoundé, Cameroon

M. M. Faye

Univ. Cheikh Anta Diop de Dakar
BP 5005 Dakar – Fann, Sénégal

We consider the shock type wave solution of the modified quintic complex Ginzburg – Landau equation and make a numerical study of its spatiotemporal stability. Discussions related to the behaviour of this front wave are introduced and it is shown how the velocities of the wave could be utilized to collect information concerning the patterns formation in the system.

Для модифікованого комплексного рівняння Гінзбурга–Ландау розглянуто розв'язок типу ударної хвилі та досліджено його просторово-часову стійкість, поведінку такої фронтальної хвилі і показано яким чином застосувати швидкості хвилі для отримання інформації про структуру системи, що утворюється.

In these last years, a certain class of nonlinear partial differential equations known as evolution equations [1 – 4] has become of immense interest to theoretical physicists and mathematicians. These equations have applications in many areas of physics [5 – 9]. For fact, the quintic complex Ginzburg – Landau equation (QCGLE) is well known as a generic model for the study of weakly nonlinear waves. It arises in physical systems which involve a balance between nonlinearity and dispersion near the critical points. For example, it describes the slow modulations of an oscillatory mode close to a subcritical bifurcation [10]. Many other applications of this equation exist, such as patterns formation [11] and thermodynamic potentials [12] in nonequilibrium systems, Benjamin – Feir turbulence in convective binary fluid mixture [13], subcritical bifurcations to counter propagating waves [14] to name only few. However, to include other relevant phenomena namely inhomogeneity, dissipation, discreteness, and allow it to describe physical systems in which many of those contributing factors are simultaneously acting, the QCGLE has been recently replaced by the modified QCGLE [15] (MQCGLE):

$$iU_t + PU_{xx} = Q_1 |U|^2 U + Q_2 |U|^4 U + C (U_x U_x^*/U^*) + i\gamma U. \qquad (1)$$

Hereafter, we consider physical systems governed by the MQCGLE and propose to examine the motion of its possible solutions. In this equation, subscripts t and x denote partial derivatives, $U(x,t)$ is complex amplitude and the parameters P, Q_1, Q_2, C and γ are complex constants. Consequently, many types of nonlinear dispersive and dissipative effects are included in Eq. (1). Following Pelap and Faye [15], we can distinguish two main regions for the motion of a plane wave introduced in the MQCGLE that are the unstable region for $(P_rQ_{1r} + P_iQ_{1i}) - r < 0$ and the stable region that corresponds to $(P_rQ_{1r} + P_iQ_{1i}) - r > 0$ with $r = -2(P_rQ_{2r} + P_iQ_{2i})|a|^2$ in which $|a|^2$ designates the amplitude of the wave. Hence, the behaviour of solutions of Eq. (1) should be investigated in each case. Furthermore, these authors show that the MQCGLE possesses a special type of solution arising from an overall balance between the dispersive and nonlinear effects when the latter is greater than the former. This special solution known as a shock wave can be exploited to study the patterns formation and/or the spatiotemporal transition from chaotic states to coherent structures. The corresponding shocklike solution of the MQCGLE has the form [15, 16]

$$U = \frac{ae^{i(Kx-\Omega t)}}{\left[1+e^{-2\mu(x-\eta t)}\right]^{\frac{1}{2}+i\alpha}} \tag{2}$$

where a is a complex quantity defined by

$$|a|^2 = 2\mu\sqrt{Z} \tag{3}$$

with

$$Z = \frac{1}{|Q_2|^2}\left[\left(\alpha^2-\frac{3}{4}\right)(P_rQ_{2r}+P_iQ_{2i}) + 2\alpha(P_iQ_{2r}-P_rQ_{2i}) + \left(\alpha^2+\frac{1}{4}\right)(C_rQ_{2r}+C_iQ_{2i})\right], \tag{4}$$

$$K = -\frac{1}{A_0}\left[(1+4\alpha^2)P_r + 4Z(Q_{2r}+2\alpha Q_{2i})\right]\mu - \frac{1}{A_0}(Q_{1r}+2\alpha Q_{1i})\sqrt{Z} = e\mu + d, \tag{5a}$$

$$\eta = 4\left[\left(\alpha+\frac{e}{2}\right)P_r - \left(\alpha^2+e\alpha-\frac{1}{4}\right)P_i - Q_{2i}Z + \left(\alpha^2+e\alpha+\frac{1}{4}\right)C_i\right]\mu + 2(P_r-2\alpha P_i)d - 2Q_{1i}\sqrt{Z} - 4\alpha C_i d, \tag{5b}$$

$$\Omega = \left[(P_r+C_r)e^2 + 4Q_{2r}Z\right]\mu^2 + 2\left[(P_r+C_r)ed + Q_{1r}\sqrt{Z}\right]\mu + \left[\gamma_i + (P_r+C_r)d\right], \tag{5c}$$

$$\mu = A_1 \pm \sqrt{A_1^2 + A_2}, \tag{6}$$

where

$$A_0 = (1+4\alpha^2)P_i + 2\alpha(C_r+2\alpha C_i), \qquad A_1 = -\frac{\left[(P_i+C_i)ed + Q_{1i}\sqrt{Z}\right]}{A_3},$$

$$A_2 = \frac{\left[\gamma_r - (P_i+C_i)d^2\right]}{A_3}, \qquad A_3 = (P_i+C_i)e^2 + 4Q_{2i}\sqrt{Z}.$$

In these relations, we have set

$$\alpha = \beta \pm \left(\beta^2 + 3/4\right)^{\frac{1}{2}} \quad \text{wherein} \quad \beta = \frac{P_r Q_{2r} + P_i Q_{2i}}{P_i Q_{2r} - P_r Q_{2i}}. \tag{7}$$

It follows from the expression (3) that Z should always be taken positive so that $|a|^2 > 0$ by making a proper choice of the branch of α.

The most interesting question about fronts is their dynamical behaviour as solutions of Eq. (1), namely their stability and the case with which they can be reached from given initial conditions. In order to fit the mathematical ansatz with physical sense, we must consider its stability as an important query. Therefore, it becomes worth while to examine the spatiotemporal stability of the solution (2) in the framework of the MQCGLE. Since computations that lead to the analytical expression (2) are hard, the numerical approach is selected for our investigation. The integration of Eq. (1) is performed using the fourth-order Runge – Kutta scheme. In the numerical simulations, we consider a system of $N = 700$ sites with infinite boundary conditions at the two ends of the chain. The step sizes are taken to be $\Delta t = 0.055$ and $\Delta x = 0.5$. The variables t and x are measured in units of time and space, respectively. During this analysis, only the branch α_+ is used, $|a|^2 = 1$, and the coefficients of the MQCGLE are

$$\begin{gathered} P_r = +1, \quad P_i = -2.2, \quad Q_{1r} = +1, \quad Q_{1i} = -0.77, \quad C_r = -0.55, \quad C_i = 0.8, \\ \gamma_r = 2.0, \quad \gamma_i = 0.0, \quad Q_{2i} = -0.5 \end{gathered} \tag{8}$$

with unfixed values for the coefficient Q_{2r}.

Before progressing, it should be stressed that the term $C\left(U_x U_x^*/U^*\right) = C\left(|U_x|^2 U/|U|^2\right)$ present in the MQCGLE tends to the infinity as $|U| \to 0$. Then it is obvious to take into account such a term only in the presence of the amplitude field, i.e., for $|U| \neq 0$. Numerically, this is materialized by $|U| > \varepsilon$ where $\varepsilon << 1$. For instance, we choose $\varepsilon = 10^{-5}$ to avoid the infinite amplitude which has no physical meaning.

To obtain the numerical results, we scrutinize the evolution of the localized initial excitation (2). Figure 1 illustrates the motion of an unstable shock wave for the coefficients defined by (8) with $Q_{2r} = -4.0$ at $t = 532$. These values correspond to a wave moving in the modulational instability domain [15] that is for $(P_r Q_{1r} + P_i Q_{1i}) - r = -3.106 < 0$. From this figure, we remark that there exists a selected pattern which propagates in the finite amplitude state, accompanying a chaotic region. Hence, we note the coexistence of a coherent structure with a chaotic state and these two distinct structures are separated by a sharp interface. It should be mentioned that similar results have been obtained for the complex Ginzburg – Landau equation [16] (CGLE) which corresponds to the particular case of Eq. (1) where $C = Q_2 = 0$ and γ real. Besides these results, we have the graph of Fig. 2 which describes the propagation of the stable shock wave for the parameters (8) with $Q_{2r} = -0.75$ at $t = 532$. These values of the constants deal with the modulational stability case [15], i.e., $(P_r Q_{1r} + P_i Q_{1i}) - r = 3.394 > 0$. Only one spatial pattern moves in the system.

In the following, we introduce another approach that helps to understand the transition from the chaotic state to the coherent structure during during the evolution of a packet wave in the system. It also permits to explain the patterns formation in the network. This new analysis is based on the comparison of the velocity of the front of the chaos (V_{ch}) and the velocity of the

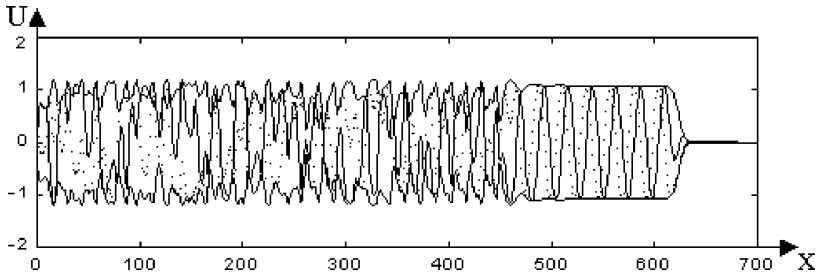

Fig. 1. Propagation of the unstable shocklike solution of Eq. (1) with the constants $P_r = +1$, $P_i = -2.2$, $Q_{1r} = +1$, $Q_{1i} = -0.77$, $C_r = -0.55$, $C_i = 0.8$, $\gamma_r = 2.0$, $\gamma_i = 0.0$, $Q_{2i} = -0.5$, where $Q_{2r} = -4.0$ and $t = 532$. Here, a chaotic structure and a coherent state coexist and travel together.

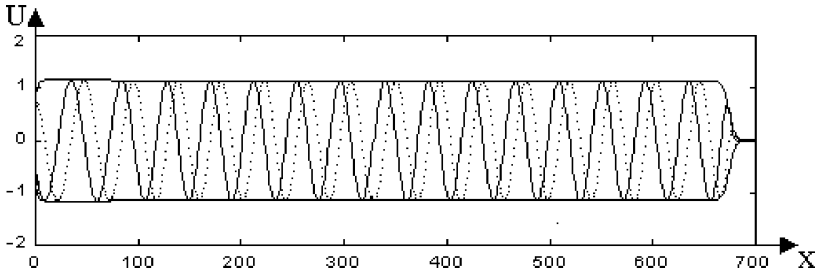

Fig. 2. Motion of the stable shocklike solution of Eq. (1) for the parameters of Fig. 1 in which $Q_{2r} = -0.75$. Solid curve corresponds to the real part of $U(x,t)$ and the dashed curve stands for its imaginary part.

front of the shock wave ($V_{\rm num}$). These two velocities are evaluated numerically throughout the simulations and their representations as function of the coefficient Q_{2r} and are shown on Fig. 3. This figure reveals that $V_{\rm ch}$ decreases and tends to zero with the increment of Q_{2r}. It implies the total disappearance of the chaotic state (i.e., the instability regime) in the system and the return to a coherent and stable state. We could also note that $V_{\rm ch}$ is always less than $V_{\rm num}$. Moreover, we can simply compare the two velocities by determining their ratio $V_{\rm ch}/V_{\rm num}$ versus Q_{2r} as it is done on Fig. 4. It is deduced from the obtained plot that $V_{\rm ch}/V_{\rm num} < 1$. This result means that the front of the shock wave moves faster than the front of the chaos.

Because the front of the shock wave moves faster and faster and the chaotic state diminishes with the increment of Q_{2r}, it could arise a situation where the stable wave behind the front is unable to follow the front correctly. This situation can occur if the phase velocity $V_\phi\,(=\Omega/K)$ is not adapted to the velocity of propagation of the front η. Indeed, for $Q_{2r} = -1.18$ we obtain the graph of Fig. 5 which shows the existence of two wavelength patterns in the system. Here, the front of the shock wave moves faster and there is a spread of the long wavelength (lw) between the selected short wavelength (sw) and the front of the shock wave. Analytically we were expected to have one wave that travels with the frequency Ω (defined by (5c)) behind the front of the shock wave. Numerically, it is verified only for a certain interval of values of Q_{2r} (sw) after what another type of wave (lw) arises and they propagate together behind the front.

This approach can be generalized by comparing all the velocities related to the solution (2), namely, the velocities (η,$V_{\rm num}$) of the front of the shock wave, the velocity of the phase V_ϕ, and the velocity of the front of the chaos $V_{\rm ch}$. The quantities η and V_ϕ are evaluated analytically

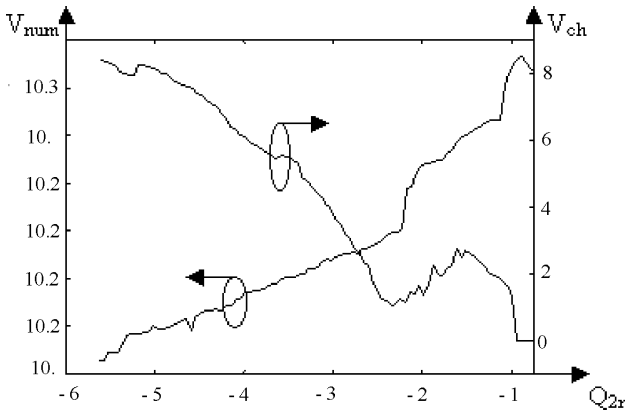

Fig. 3. Velocities of the front of the chaos ($V_{\rm ch}$) and that of the shock wave ($V_{\rm num}$) vs the parameter Q_{2r}. The velocity $V_{\rm ch}$ decreases and tends to zero when Q_{2r} increases while $V_{\rm num}$ increases with Q_{2r}.

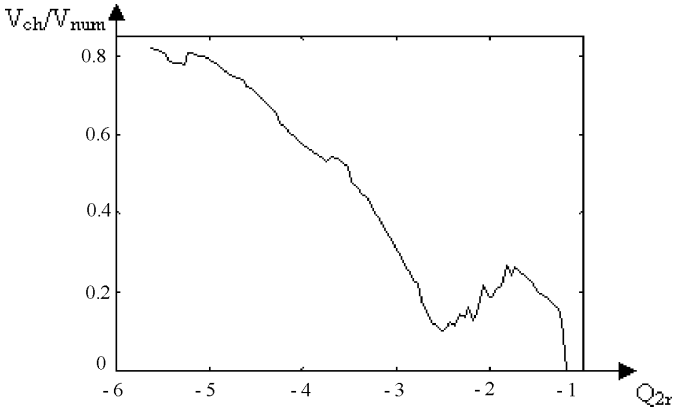

Fig. 4. Ration $V_{\rm ch}/V_{\rm num}$ as function of Q_{2r}.

from relations (5) while $V_{\rm num}$ and $V_{\rm ch}$ are calculated numerically during the simulations. Figure 6 presents different profiles of the ratios of those velocities in terms of Q_{2r} and incites to make some comments. First, the ratio $V_{\rm num}/V_\phi$ is a decreasing function of Q_{2r} but takes values that remain bigger than 1 showing that $V_{\rm num}$ is always greater than V_ϕ. This mayor difference between $V_{\rm num}$ and V_ϕ suggests that there could exist many types of structures evolving behind the front (for e.g., report to Fig. 5). Next, we deduce from Fig. 6 that the ratio $V_{\rm num}/\eta$ is a constant function of Q_{2r} except for the value $Q_{2r} = -1.18$. Third, we also note from this last figure that η/V_ϕ decreases at the left of $Q_{2r} = -1.18$ and increases at its right. Then it becomes of interest to seek the behaviour of (2) for this particular value of Q_{2r}. The investigation leads to the graph of Fig. 5.

In this paper, the MQCGLE that described wave propagations and phase transitions in many nonequilibrium systems has been considered and the stability of its shock wave solution investigated numerically. We have shown that the dynamical behaviour of this solution strongly depends on the contribution of the quintic term Q_2 within Eq. (1). It has appeared from the behaviours of the velocities of the solution (2) versus Q_{2r} that the velocity of the front of the

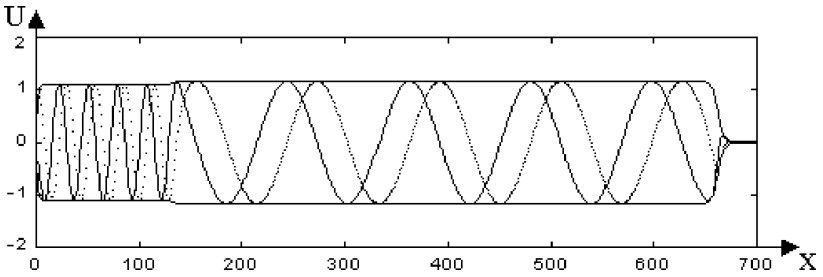

Fig. 5. Evolution of the stable shocklike solution of Eq. (1) for the particular value $Q_{2r} = -1.18$ and the constants of Fig. 1. Here, the system comprises two wavelength patterns (sw and lw) that evolve together behind the front of the shock wave. At the same time, we note a slight variation of the wave amplitude in a vicinity of the transition between the different wavelength states.

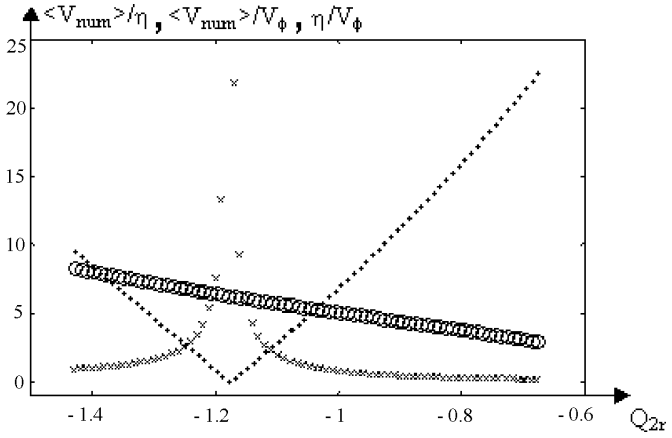

Fig. 6. Ratios $V_{\rm num}/\eta$, $V_{\rm num}/V_\phi$ and η/V_ϕ as function of Q_{2r}. The other parameters are taken to be $P_r = -1$, $P_i = -2.2$, $Q_{1r} = +1$, $Q_{1i} = -0.77$, $C_r = 2.24$, $C_i = 0.8$, $\gamma_r = 2.0$, $\gamma_i = 0.0$, $Q_{2i} = -0.5$. We have the cross (xx) for $V_{\rm num}/\eta$; the circle (oo) for $V_{\rm num}/V_\phi$ and the dashed line (–) for η/V_ϕ. Each curve has a smooth evolution for the diverse values of Q_{2r} except $Q_{2r} = -1.18$ at where this behaviour is broken.

chaos decreases and tends to zero with the growth of Q_{2r}. As an outcome, we have deduced that the instability region for the propagation of (2) could be avoided by making a good choice of the domain of values of Q_{2r}. It has also appeared from this study that the behaviours of the ratios of diverse velocities of the solution could inform a lot on the spatial patterns formation in physical systems governed by the MQCGLE.

1. *Ames W. F.* Nonlinear partial differential equations in engineering. – New York: Acad. Press, 1965, 1967. – Vols 1, 2.
2. *Lax P. D.* Integrals of nonlinear equations for evolution and solitary waves // Communs Pure and Appl. Math. – 1968. – **21**. – P. 467 – 490.
3. *Dodd R. K., Eilbeck J. C., Gibbon J. D., Morris H. C.* Solitons and nonlinear wave equations. – London: Academic, 1987.
4. *Hegseth J. J., Andereck C. D., Hayot F., Pomeau Y.* Spiral turbulences and phase dynamics // Phys. Rev. Lett. – 1989. – **62**. – P. 257 – 260.

5. *Benjamin T. B., Feir J. F.* The disintegration of wave trains on deep water // J. Fluid Mech. – 1967. – **27**. – P. 417 – 430.
6. *Kuramoto K.* Prog. Theor. Phys. – 1976. – **56**. – P. 679.
7. *Bekki N.* Nonlinear modulation of ionization waves // J. Phys. Soc. Jap. – 1981. – **50**. – P. 659 – 667.
8. *Agrawal G. P.* Nonlinear fiber optics. – New York: Acad. Press, 1995.
9. *Pelap F. B., Kofané T. C., Flytzanis N., Remoissenet M.* Waves modulations in the biinductance transmission line // J. Phys. Soc. Jap. – 2001. – **70**. – P. 2568 – 2577.
10. *Pomeau Y.* Front motion, metastability and structural bifurcations in hydrodynamics // Physica D. – 1986. – **23**. – P. 3 – 11.
11. *Niemela J. J., Ahlers G., Cannell D.* Phys. Rev. Lett. – 1990. – **64**. – P. 1365.
12. *Descalzi O., Martinez S., Tirapegui E.* Thermodynamic potentials for non-equilibrium systems // Chaos, Solitons and Fractals. – 2001. – **12**. – P. 2619 – 2630.
13. *Brand H. R., Lomdahl P. S., Newell A. C.* Benjamin – Feir turbulence in convective binary fluid mixture // Physica D. – 1986. – **23**. – P. 345 – 361.
14. *Deissler R. J.* J. Stat. Phys. – 1989. – **54**. – P. 1459.
15. *Pelap F. B., Faye M. M.* Modulational instability and exact solutions of the modified quintic complex Ginzburg – Landau equation // J. Phys. A: Math. and Gen. – 2004. – **37**. – P. 1727 – 1735.
16. *Nozaki K., Bekki N.* Pattern selection and spatiotemporal transition to chaos in the Ginzburg – Landau equation // Phys. Rev. Lett. – 1983. – **51**. – P. 2171 – 2174.

Received 29.04.2004